A PHENOTYPIC STUDY OF INTRAFLAGELLAR TRANSPORT AND FLA10 IN THE *lf4* MUTANT OF *CHLAMYDOMONAS REINHARDTII*

By

KEVIN M. PARGETER

Bachelor of Science in Biology

University of Central Oklahoma

Edmond, Oklahoma

2004

Submitted to the Faculty of the
Graduate College of the
Oklahoma State University
in partial fulfillment of
the requirements for
the Degree of
MASTER OF SCIENCE
May 2009

A PHENOTYPIC STUDY OF INTRAFLAGELLAR TRANSPORT AND FLA10 IN THE *lf4* MUTANT OF *CHLAMYDOMONAS REINHARDTII*

Thesis Approved:

William D. Meek, Ph.D., Thesis Adviser

Nedra F. Wilson, Ph.D.

Kenneth E. Miller, Ph.D.

A. Gordon Emslie, Ph.D.
Dean of the Graduate College

ACKNOWLEDGMENTS

The opportunity to study and obtain my education would not have been possible without the love and support from my parents Terry and Carolyn Pargeter, whose encouragement has been invaluable to me. Additionally, my two brothers and three sisters have been lifelong friends, and, despite my long absences to pursue higher education, are my strongest of supporters. I am deeply thankful for the generous support of my uncle Russ Goodno, Ph.D., and aunt Judy Goodno who helped pay for my undergraduate tuition. To all my family, I dedicate this work.

Special thanks go to Dr. Bill Meek, Dr. Nedra Wilson and Dr. Kenneth Miller at Oklahoma State University Center for Health Sciences (OSU-CHS) who guided me through my studies of a fascinating organism *Chlamydomonas reinhardtii*. Plus, I am indebted to all the faculty and staff at OSU-CHS who have helped me in this endeavor, especially Jeff McCosh, Oza McClain and Julie Buchheim. Thank you all for your past and future direction.

TABLE OF CONTENTS

Chapter **Page**

LIST OF FIGURES

Item **Page**

LIST OF TABLES

Item **Page**

LIST OF ABBREVIATIONS

CHO	Chinese hamster ovary
EtOH	ethyl alcohol
FLA10p	Flagellar length assembly protein 10
H	hour
IFT	Intraflagellar transport
IMCD	inner medullary collecting duct
IMF	Immunofluorescence
LF4	*long-flagellar* gene 4
lf4	long flagellar phenotype 4
LF4p	long flagellar protein 4
Min	Minute(s)
NBF	normal buffered formalin
NHS	normal horse serum
PBS	phosphate buffered saline
PBS-T	phosphate buffered saline with 0.1% Tween-20
PCD	primary ciliary dyskinesia
PKD	polycystic kidney disease
RT	room temperature
SEM	scanning electron microscopy
TEM	transmission electron microscopy
UA	uranyl acetate
WISH	Wistar Institute Susan Hayflick cell line

CHAPTER I

INTRODUCTION

Background

Flagella are long, hair-like projections involved in cellular locomotion, in contrast to cilia, which are patches of hair-like projections that coat the free surface of vertebrate cells. Several similarities exist between cilia and flagella: (1) they are both covered by cell membranes; (2) they possess remarkably similar internal cytoskeletons, known as the 9+2 arrangement of microtubules in flagella and cilia or the 9+0 arrangement in primary cilia; (3) they possess many homologous proteins that are conserved throughout nature (Pazour and Witman, 2008); and (4) they are both anchored into cells with proximal, intracellular basal bodies (Geimer and Melkonian, 2004). In mammals, flagella are important motile structures for spermatozoa, but otherwise are rarely found in the architecture of stationary cells. Cilia, on the other hand, cover the apical surfaces of respiratory cells in the upper airways and in cells of the Fallopian tube, where they function to sweep material or ova along passageways, respectively. A single nonmotile cilium, also called a primary cilium, can be found on almost all cells in the human body at some point during cellular development (Michaud and Yoder, 2006). As reviewed by Pan and Snell (2002), the primary cilium has a sensory function, for example, the photoreceptor in vision or chemoreceptor in olfaction. Moreover, the presence of primary cilia in the kidney was initially reported over a hundred years ago (Zimmerman, 1898), but not until recently has this organelle been recognized as more than a vestigial

appendage. Primary cilia are found even within bone (Malone, 2007) and on the corneal epithelium (Figure 1). Many of the cellular mechanisms that operate in cilia are found and operate in flagella and, by studying flagella, one can learn more about the nature of cilia (Pan and Snell, 2005).

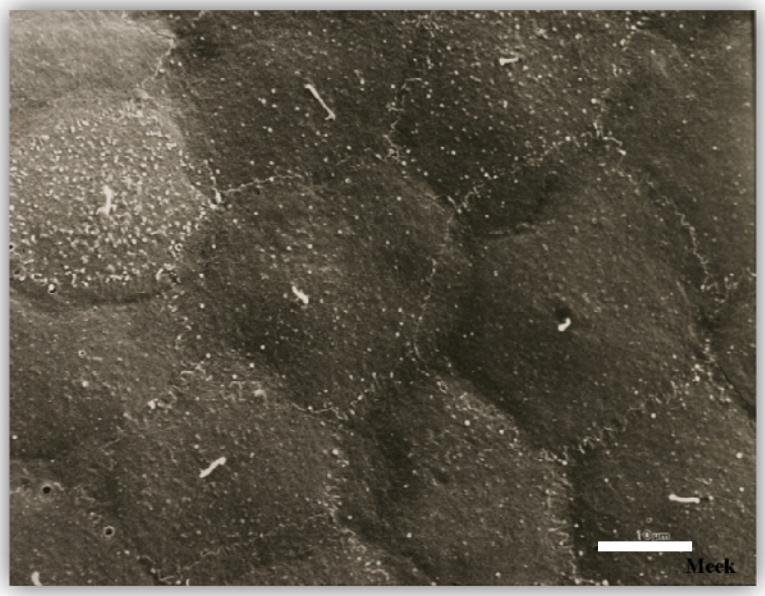

***Figure 1*:** SEM of ciliated rabbit corneal epithelium. Note the single cilium evident near the central portion of most cells. The cells are circular in shape and cell boundaries appear in a scalloped pattern. Microvilli are also present on some of the cells. Primary cilia appear much longer than the microvilli (Meek, unpublished). Bar is 10 µm.

Humanity suffers several disorders of cilia, such as polycystic kidney disease (PKD) and primary ciliary dyskinesia (PCD) as reviewed by Asleson and Lefebvre (1998). These disorders occur when there is a loss of the tightly-controlled ciliary assembly. To facilitate research, the basic science community sought and found a simple model to study ciliary pathologies by using the unicellular green alga organism *Chlamydomonas reinhardtii*. In Greek, *Chlamys* means cloak and *monas* means solitary (Harris, 2008a). This name describes two properties of *C. reinhardtii*, the cell wall

(cloak) and the unicellular (solitary) nature. The basic attributes of *C. reinhardtii*, such as its biflagellate and unicellular state plus the ease of which to culture it, represent great opportunities for analysis into flagellar and ciliary function and dysfunction, which strengthens the role this organism can play in basic science compared to other common model organisms (Table 1). The genes for structural proteins in *C. reinhardtii* are remarkably homologous to human ciliary genes, which has facilitated the groundwork for understanding PCD (Pazour, 2008). Additionally, *C. reinhardtii* has been reported as the ideal organism for investigations on flagellar length control (Nguyen et al., 2004). Therefore, studying *C. reinhardtii* offers tremendous scientific importance in understanding how cells regulate organelle size and may help explain a multitude of disorders.

	Biochemically Characterized	**Genome**	**Proteome**	**Flagella/Cilia nonessential**	**Ease of Flagella/Cilia Isolation**	**Mutants Available**
Mus musculus	+/++	+++	++	-	-/+	+
Sea Urchin	+/++	-	-	?	+++	?
C. elegans	+/++	+++	-	++	-/+	++
Chlamydomonas	+++	+++	+++	+++	+++	+++

***Table 1*:** Properties of *Chlamydomonas* compared to other model organisms. *Chlamydomonas* can be argued as the most suited organism to study cilia. +++, ideal; ++, good; +, poor; -, not usable; ?, unknown.

Past studies have shown flagellar assembly relies and/or depends on a mechanism called intraflagellar transport (IFT) (Kozminski et al., 1993). IFT involves a motor protein called kinesin-II, which travels in a zipper-like manner along the microtubule cytoskeleton away from the cell body and out into flagella towards the plus end of microtubules. The kinesin-II homolog in *C. reinhardtii* is FLA10p (Flagellar Length

Assembly protein 10). FLA10p carries the axoneme precursors involved in the assembly of flagella (Qin, 2004) to the flagellar tip, where precursors are exchanged for old particles and shuttled via a separate motor protein called cytoplasmic dynein back to the cell body for breakdown as reviewed by Pederson and Rosenbaum (2008). There are four *long-flagella* genes that have been implicated in recent studies that play a role in the regulation of length control (Asleson and Lefebvre, 1998). The mutants of these genes, known as *lf1*, *lf2*, *lf3*, and *lf4*, are reported to be necessary for normal flagellar length regulation, yet, a full explanation of flagellar control of length remains incomplete (Wilson et al., 2008).

Within the *lf4* phenotype, little is known as to the exact location of FLA10p, whereby localizing FLA10p would not only further explain the morphology of this important *long-flagella* mutant but should further facilitate our understanding of FLA10p in flagellar length control. Therefore, the purpose of this study involved the phenotypic characterization, or in other words, a description of observable microscopic features of the cells and flagella of *lf4*. And due to the lack of previous ultrastructural studies of *lf4*, I sought to systematically characterize this mutant using a number of microscopic methods including bright-field, immunofluorescence (IMF), scanning electron microscopy (SEM) and transmission electron microscopy (TEM). In addition, I have used TEM to quantify the number of IFT particles in wild-type and *lf4* flagella.

This qualitative characterization of *lf4* should facilitate our understanding in how flagellar size is regulated, which in turn should contribute to the growing field of translational research on human ciliary disorders. The fields of medicine and biomedical

science will incrementally benefit, perhaps indirectly, from this phenotypic characterization of *lf4* flagella.

CHAPTER II

REVIEW OF LITERATURE

Intraflagellar Transport

The ground breaking discovery by Kozminski et al. (1993) of a motility within flagella called intraflagellar transport (IFT) revolutionized our understanding of ciliary and flagellar assembly. This study utilized video and electron microscopy to demonstrate the role of FLA10p and IFT in assembly and disassembly of flagella. This initial investigation and report on IFT spawned a new field and has laid the groundwork for understanding the mechanisms that underlie ciliopathies.

FLA10p moves IFT particles, the shape of which varies from small lollipop-like structures to large rafts that contain 17-18 or more individual particles and are found between the flagellar membrane and the outer-doublet microtubules (Kozminski et al, 1993). In addition to determining the presence of FLA10p, later papers reported how FLA10p functions in IFT, which transports cargo destined for incorporation into flagella along the axoneme microtubules much as a truck carries parts on a highway (Qui et al., 2004).

During the same time as the initial IFT and FLA10p studies, the first characterization of mutants defective in the ability to regulate the length of flagella were reported in 1998 by Asleson and Lefebvre. These authors described the genetics of *long-flagella* loci and the identification of the *lf4* mutant. In this study they determined the

mean lengths of *long-flagella*, which are two to three times the length of wild-type flagella.

It was not always apparent how flagella regulated the transport of IFT cargo and regulated the assembly of flagella at a pre-set length. The mechanism of IFT was known, but how did flagella establish a length? Marshall and coworkers (2005) described a balance-point model to explain how lengths of organelles in general and in flagella in particular were controlled. It involved the addition of precursors by FLA10p and removal of turn-over particles with cytoplasmic dynein in a steady-state process. He also reported that IFT protein quantity versus flagellar length operated independently. Marshall did not measure the number of IFT particles per flagellar length using TEM images, as reported in this work.

Long Flagella Specifics and Techniques

Several studies have focused on aspects of FLA10p and its role in IFT (Marshall and Rosenbaum, 2001) for the proper length regulation of flagella. Flagella continually are turning over, and in the absence of a mechanism to replace proteins that are lost due to turnover, flagella disassembly exceeds flagellar assembly and therefore becomes progressively shorter. Marshall and Rosenbaum (2001) reported that IFT was essential for flagellar assembly and maintenance and was necessary for regulation of length. Subsequently, it was found that a novel mitogen-activated protein (MAP) kinase was "crucial" in determining the length of *lf4* flagella (Berman et al., 2003). Here, I will report on the first ultrastructural characterization of *lf4* flagella. Moreover, biochemical studies of *lf4* flagella demonstrated a significant increase in FLA10p levels compared to wild-type flagella (Wilson and Lefebvre, unpublished observations). To this end, I have

localized FLA10p in both wild-type and *lf4* using IMF. These studies may help decipher the molecular mechanisms that regulate the length and assembly of flagella. This study will specifically aim to describe: (1) the morphology of the *lf4* phenotype using bright-field, scanning, and transmission electron microscopy; and (2) the localization of FLA10p in the *lf4* mutant using immunofluorescent microscopy. Furthermore, IFT particles will be counted and compared in wild-type and *lf4* per flagellar length, area, and volume. It is hypothesized that the IFT particle quantity will be independent of length in *lf4*, just as Marshall (2005) reported in other *Chlamydomonas* mutants.

CHAPTER III

METHODS AND MATERIALS

The research design and methodology employed cell culture techniques using *C. reinhardtii* and three mammalian cell lines, plus bright-field, immunofluorescence, scanning, and transmission electron microscopy.

Chlamydomonas Cultures

Strains of *C. reinhardtii* utilized included the wild-type (CC-1690 mt^+ 21gr) and *lf4* mutants, such as *lf4-1 arg7-*, *lf4-3 arg7-*, *lf4-6* and *lf4-10*. These strains were graciously provided by Dr. Nedra Wilson of Oklahoma State University Center for Health Sciences (OSU-CHS). Cells were maintained on TAP agar plates and transferred to liquid cultures consisting of Medium II (Gorman and Levine, 1965). Cells were grown under a 13:11 hour (h) light:dark cycle at 22^{o}C with mild to moderate aeration. Some *lf4* mutants, such as *lf4-6*, required supplementation with exogenous arginine (Sager and Granick, 1954).

The time period of growth and other factors was determined by preliminary experiments involving wild-type and *lf4* mutants. After inoculating the liquid media, all strains were observed and video recorded (Appendix A) at successive time points of 12, 24, 36, and 48 h. As flagella are required for cell motility, I used an estimate of overall swimming activity as a determinant of the flagellated status of cells (Mueller et al., 2005). Briefly, all strains were analyzed by viewing an aliquot of cells on a pre-cleaned glass microscope slide (Anapath, Lewisville, TX), at 40x with a standard laboratory

dissecting microscope. Based on a gross observation, the cell swimming activity was estimated. Wild-type and *lf4* cell activity were both judged at the same setting and on the same brand of glass slides. A high-definition digital video camera (Insignia/Best Buy, Richfield, MN) was positioned close to the microscope eye piece and used to film the estimated swimming activity.

Mammalian Cell Cultures

Chinese hamster ovary (CHO) cells (Puck et al., 1958), inner medullary collecting duct (IMCD) cells (Rauchman et al., 1993), and WISH (Wistar Institute Susan Hayflick), a human amnion epithelial cell line (Hayflick, 1961; Meek and Davis, 1986) were grown in a Forma Scientific incubator in humidified 95% air and 5% CO_2 gas at 37^{o}C. The CHO and WISH were purchased from the American Type Culture Collection (Manassas, VA) and the IMCD cells were graciously provided by Dr. Rashmi Kaul of OSU-CHS. Standard culture mediums for the respective cell lines were used (Hayflick, 1961; Meek and Davis, 1986). The media was supplemented with fetal calf serum (Atlanta Biologicals, Lawrenceville, GA) and antibiotic/antimycotic solutions (Gibco, Grand Island, NY). Either CHO, IMCD or WISH cell lines were processed concurrent with *C. reinhardtii* to act as experimental controls.

Bright-field Microscopy

Using either a Nikon Labophot microscope (Tokyo, Japan) with a Sony Color Digital Camera (Tokyo, Japan) or a Zeiss Photomicroscope III (Peabody, MA) with Spot Camera software (Diagnostic Instruments, Sterling Heights, MI), cells were viewed and images captured under bright-field microscopy to ensure flagellation prior to processing

for IMF, SEM, and TEM. To fix and preserve cells, Lugol's iodine (4% iodine crystals, 6% potassium iodide) was applied prior to image capture (Caprette, 1996).

Immunofluorescence Microscopy

A procedure for indirect immunofluorescence (IMF) was formulated based on previously published methods (Carson et al., 1973; Huang et al., 1988; Cole et al., 1998). In addition, the gene product of *LF4*, LF4p, was examined in wild-type and *lf4* mutants.

Frosted, pre-cleaned, microscope slides (Anapath) were etched with three equidistant circular wells per slide, and treated with a 1:10 dilution of poly-$_L$-lysine (Sigma, St. Louis, MO). In addition, 12-well slides were utilized as well (Cel-Line/Erie Scientific Co., Madison, WI). Two methods of fixation was utilized. For method 1, in 12 mL Falcon tubes (BD Falcon, Franklin Lakes, NJ), cells were fixed for 10 minute (min) with Carson's normal buffered formalin (NBF) at 3.7% (Carson et al., 1973). For method 2, cells were fixed for 10 min in paraformaldehyde 1.5% (Cole et al., 1998). Other than fixation, the methods are the same. Cells were centrifuged at 750 revolutions per minute (RPM) for three to four min on an IEC Clinical Centrifuge (Damon, Needham, MA) and washed with phosphate buffered saline (PBS) containing 0.3% Triton X-100 (Sigma) at pH 7.2 (Miller et al., 2002). In humidified chambers at room temperature (RT), a 20 µL aliquot of cells was transferred to slides and allowed to adhere for 10 to 15 min. Cells were permeabilized in Coplin jars containing either 0.5% NP-40 for two min at RT or -20^{o}C 100% methanol for 10 min. For *Chlamydomonas* cells, chlorophyll extraction occurred with fresh -20^{o}C acetone for 8 to 10 min and slides were washed in PBS. Cells were incubated for one hour with blocking buffer containing 10mM $KHPO_4$, pH 7.2, 5% normal horse serum (NHS) (Jackson ImmunoResearch, West Grove, PA), 5% glycerol

and 1% coldwater fish gelatin (Cole et al., 1998). Primary antibodies were diluted in blocking buffer at 1:500 for the monoclonal anti-α-tubulin (Sigma); at 1:50 for LF4p (PAS403; Dr. Nedra Wilson, OSU-CHS); at 1:100 for K2.4 (Covance, Emeryville, CA), an anti-kinesin-II motor subunit that is homologous to FLA10p. Primary antibodies were allowed to incubate for one hour at 37^{o}C or overnight at 4^{o}C. Control slides were incubated simultaneously under the same conditions in equal volumes of blocking buffer only (Harlow and Lane, 1988). Slides were washed three times for five minutes each in PBS and labeled for one hour in a humidified jacket at 37^{o}C with secondary antibody. Secondary antibodies included Alexa Fluor 488 (Invitrogen, Eugene, OR) diluted 1:200 or 1:500 and Cy3 (Jackson ImmunoResearch) diluted 1:1000. The Cy3-labeled secondary antibody was graciously provided by Dr. Kenneth Miller of OSU-CHS. Slides were washed and cover-slips apposed with Prolong Gold anti-fade reagent (Invitrogen) and sealed with clear nail polish. Images were captured on an Olympus X51 fluorescent research microscope (Olympus, Center Valley, PA) with Spot Camera software (Diagnostic Instruments) and analyzed when necessary with Image J software (NIH).

Scanning electron microscopy

10 mL of *lf4-10* and wild-type cells were harvested by centrifugation and re-suspended in the primary fixative of 2.0% glutaraldehyde with 0.1M cacodylate buffer (pH 7.2-7.3) for 20 min at RT. The suspension was centrifuged and re-suspended for washing in a 0.1M cacodylate buffer. An aliquot of cells was placed on a round, glass coverslip, 12 mm in diameter (Anapath), which was previously coated with 0.1% aqueous polyethyleneamine (Sigma) to which the cells were allowed to adhere for 10-15 min. The coverslips were washed in PBS and post-fixed with 1% osmium tetroxide in

0.1M cacodylate buffer. Cells were washed and dehydrated in a graded ethyl alcohol (EtOH) series at 25%, 50%, 75%, 95% and 2 changes in 100%. The coverslips with cells attached were dried with a Denton DCP-1 Critical Point Drying Apparatus (Denton Vacuum Inc, Moorestown, NJ), placed on aluminum stubs and were coated with gold using a Polaron SC 500 Sputter Coater (Quorum Technologies, Ringmer, UK). Images were viewed on a Hitachi S-2300 (Hitachi, Pleasanton, CA) operating at 25 kV and recorded on either Polaroid 72 or Fuji ISO 400, black and white instant film.

Transmission Electron Microscopy

Wild-type and *lf4-10* mutants were prepared for transmission electron microscopy using the method of Dentler and Adams (1992). Briefly, cells were fixed for 30 min with 2% glutaraldehyde in 0.1M cacodylate buffer, pH 7.2-7.3, in 1.5 mL Micro Sample Centrifuge tubes (EMS, Ft. Washington, PA). Cells were washed, centrifuged at 750 RPM for three to four min in an IEC Clinical Centrifuge, and suspended in 3-4 mL of 0.1M cacodylate buffer. Cells were post-fixed with 1% osmium tetroxide in 0.1M sodium cacodylate for 20 min and washed briefly in 20% EtOH. Cells were stained *en bloc* with 20% EtOH/uranyl acetate for 20 min at RT and dehydrated in a graded EtOH series for 10 min two times each at 50%, 70%, 90% and 100%. Cells were cleared with propylene oxide, embedded in Epon 812 (EMS) under vacuum and polymerized at 68^{o}C for 18 h. Thin sections were cut with an Ultracut E Microtome (Reichert-Jung/Leica, Wetzlar, Germany) and viewed at 80 kV on either a Zeiss T109 Electron Microscope (Zeiss, Peabody, MA) with Gatan Digital Micrograph (Pleasanton, CA) software (see Appendix B for an instructional video on how to operate the Zeiss T109 electron microscope) or a Hitachi H7000 Electron Microscope (Hitachi, Pleasanton, CA), with a built-in large

format film camera. Negatives were processed, printed and/or scanned using standard darkroom procedures.

Quantification

Image J (NIH) was used to set scale bars for all images. For TEM micrographs, the scale bar was established using the known 25 nm diameter of a microtubule (Kierszenbaum, 2007). This method allowed for the most precise measurement of flagella and corrected for inaccuracies with magnification calibration of the electron microscope. After establishing the scale, micrographs containing flagella in either longitudinal or cross-section were analyzed by measuring flagellar diameter and length. All cross-sections were cut at a thickness of 90 nm, so 90 nm was used for the determination of volume on cross-sections. Micrographs were taken at a common magnification of 80,000x for the majority of measurements. IFT particle identification criteria included the observation of an electron-density between the outer doublet-microtubules and the flagellar membrane, and a minimum dimension of 25 nm, as based on measurements of IFT particles in Pazour (1998). The data was added to a Microsoft Excel (Redmond, WA) spreadsheet to compute area and volume. IFTs per length, area and volume were compared in wild-type versus *lf4* mutant.

CHAPTER IV

RESULTS

Bright-field Microscopic Observations

Observation of *lf4* cells revealed flagella clearly longer than wild-type (Figures 2-6). The *lf4* cells were biflagellate and structurally appeared similar to wild-type, with the flagella oriented at the apical end of the cell body. Fixation of cells with Lugol's iodine enhanced the observation of flagella and therefore the determination of whether cells were uniformly flagellated (Figure 3). Additionally, cells were observed for their estimated swimming activity, as this reflected their flagellated status (Table 2). After observing swimming activity for several days, the cultures became opaque and dark green due to large numbers of *C. reinhardtii* cells. This obstructed light from uniformly reaching other cells and led to loss of synchronization of the cell cycle. Some flagellated cells were observed as either de-flagellated or appeared motionless at all time points of observation. The *lf4-3 arg7-* and *lf4-6* mutants were the most active of the *lf4* strains at 48 h, while *lf4-10* demonstrated the least movement at all time points. Wild-type remained actively swimming at both 24 and 48 h. It was observed that the greater the initial inoculation of cells (≥ four loops) and the more vigorous aeration produced more swimming activity in less time. These cultures, however, turned opaque in only two to three days, rather than three to four days typically observed with average aeration and inoculation.

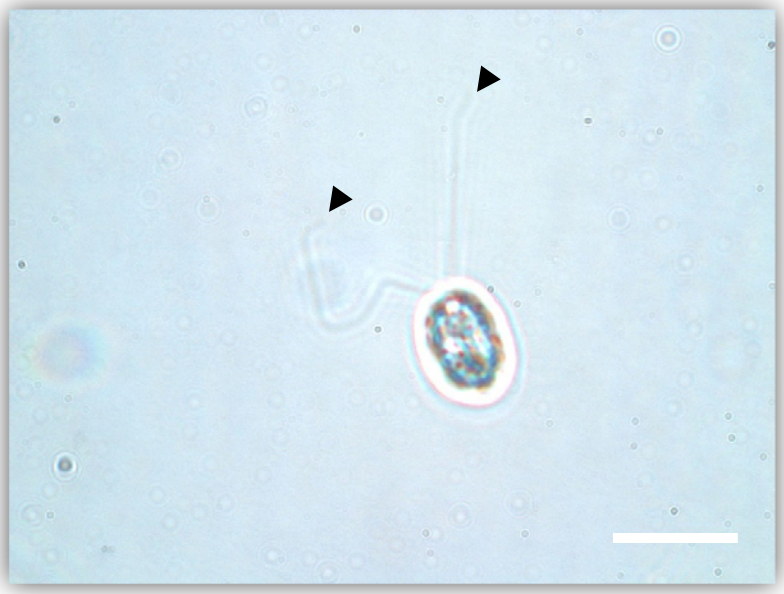

***Figure 2*:** Bright-field photomicrograph of an unstained *lf4* cell. Note that the flagella are longer than the cell body. Flagellar tips are labeled with arrowheads. Bar is 10 µm.

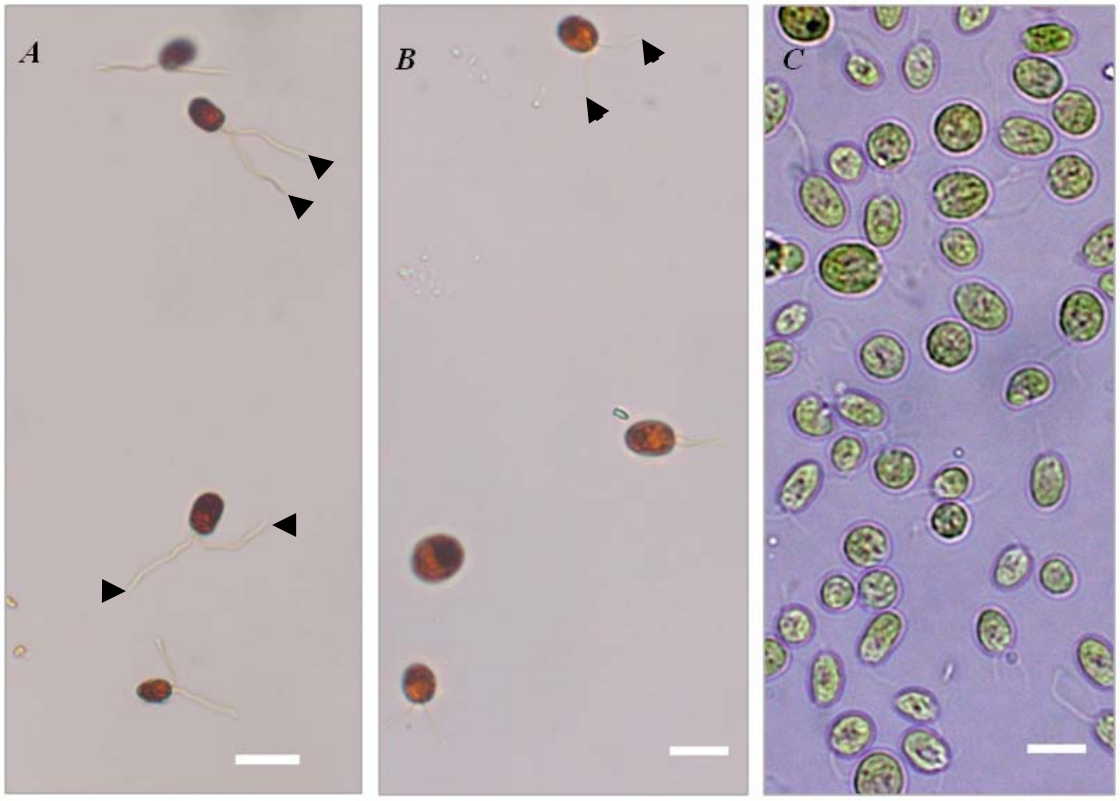

***Figure 3*:** Bright-field photomicrographs of *lf4* and wild-type cells stained with Lugol's iodine. (*A*) *lf4* with flagella that are 2-3 times the length of the cell body, and (*B*) wild-type cells stained with Lugol's iodine. Flagellar tips are labeled with arrowheads. (*C*) *lf4* cells with Lugol's iodine stain omitted. Bar is 10 µm.

	12 h	24 h	36 h	48 h
Wild-Type	++	+++	++++	+++/+
lf4-10	-	-/+	+	-
lf4-1 arg 7-	-	-/+	+	+
lf4-3 arg 7-	-	++	+/++	+/++
lf4-6	-	++	+++	++

***Table 2*:** Estimate of swimming cells per time. At 12, 24, 36 and 48 h, wild-type and *lf4* mutants are evaluated for percent of swimming activity, which indicated the presence of flagellated cells. ++++, most to all cells swimming; +++, more than majority cells swimming; ++, about half cells swimming; +, few to some cells swimming; -, little to no swimming cells.

Immunofluorescence Microscopy

As previously described by Cole and others, FLA10p localized in a punctate pattern in both the *lf4* and wild-type flagella (Figure 4, *A*-*B*; Figure 5, *A* & *E*, respectively), and had approximately equal immunoreactivity in the microscope. Tubulin localized in a linear pattern in the flagella (Figure 4, *C*). The control for FLA10p showed little to no specific staining (Figure 4, *D*). WISH and IMCD cells showed microtubules throughout the cell body and extending to the cell periphery (Figure 4, *E*; Figure 5, *F*, respectively). IMCD cells also displayed centriole staining near the central portion of many cells in a cell-cycle dependant manner. The LF4p was examined in wild-type and *lf4* mutant cells. LF4p localized in the proximal portion of wild-type in a punctate pattern (Figure 5, *B*). The *lf4* mutant appeared to have little to no specific staining for LF4p (Figure 5, *C*), however, images exhibited high background fluorescence (Figure 5, *B*-*C*). The control for LF4p showed little specific staining (Figure 5, *D*). Results with poly- and monoclonal tubulin were the same (data not shown).

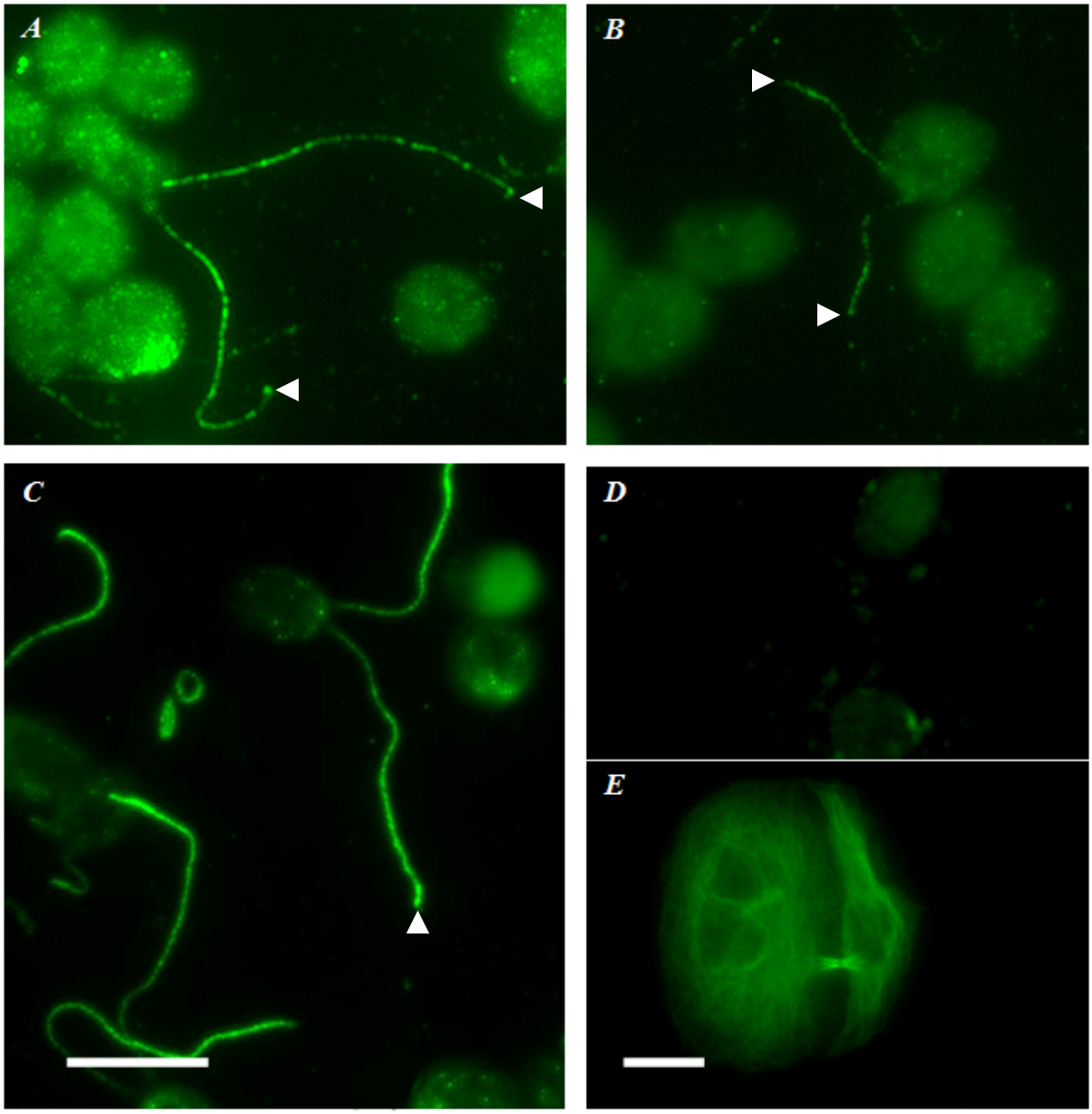

***Figure 4*:** FLA10p IMF micrographs of *lf4* and wild-type cells. (*A*) *lf4* mutant with FLA10p labeling in a punctate pattern along the flagella, (*B*) wild-type with FLA10p labeling in the same punctate pattern, (*C*) *lf4* mutant with anti-α-tubulin labeling in a linear pattern along the flagella, and (*D*) wild-type control with primary antibody omitted, showing little fluorescence. (*E*) Microtubules are distributed throughout these WISH daughter cells and are concentrated in the bright mid-body, seen between the cells. Chlorophyll autofluorescence occurs in some images. The plane of focus is set to best view flagella in all images. Flagellar tips are labeled with arrowheads. Scale bar in *A*-*D* is 10 µm; and bar is 10 µm in (*E*).

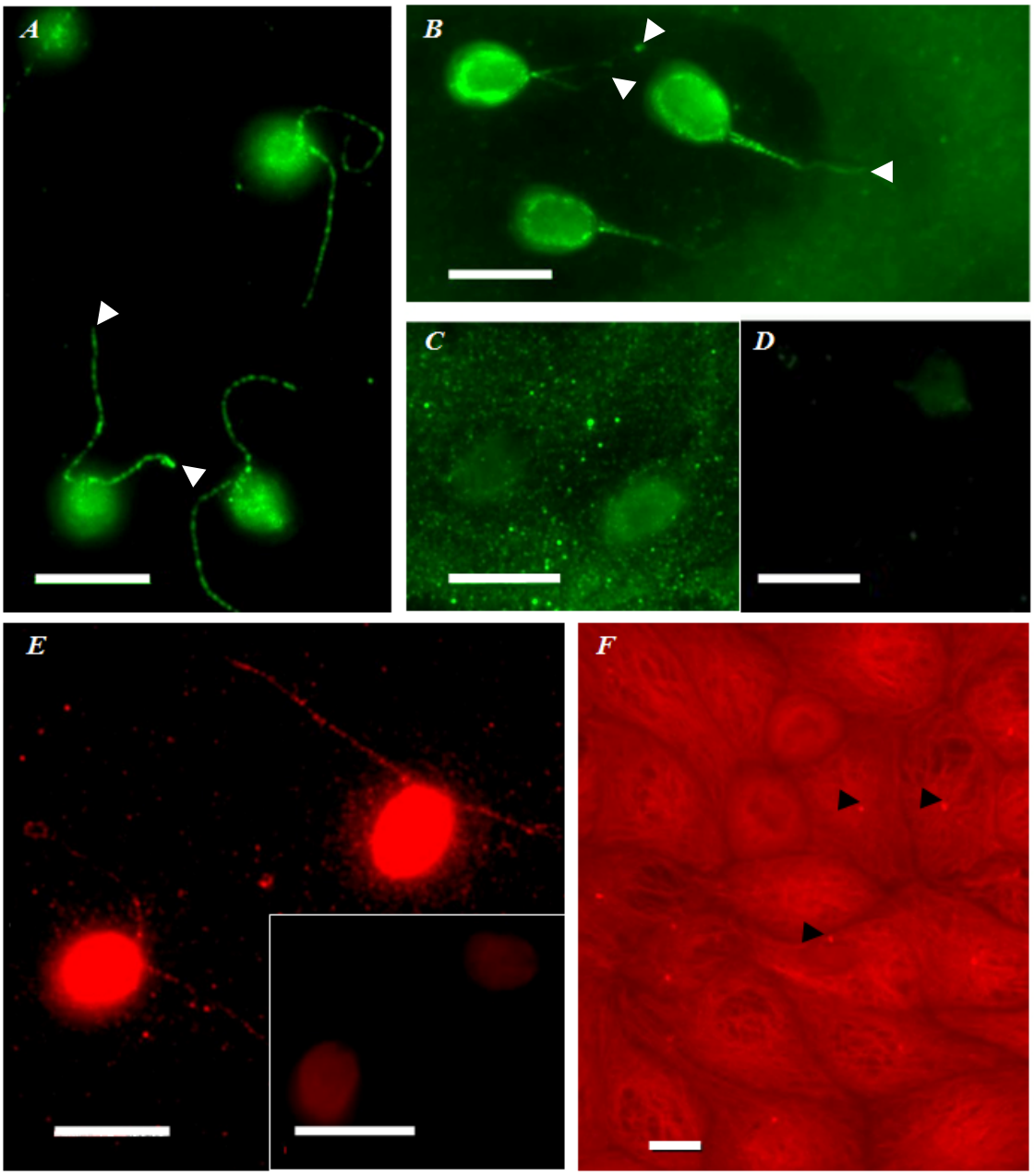

***Figure 5*:** FLA10p versus LF4p IMF micrographs of *lf4* and wild-type cells. Using Alexa Fluor 488 secondary antibodies, (*A*) *lf4* mutant labeled with FLA10p in a punctate pattern, and compares to (*B*) LF4p labeling in proximal wild-type flagella with some fluorescence in the cell body. Flagellar tips are labeled with white arrowheads. (*C*) *lf4* mutant labeled with LF4p, showing no specific staining. (*D*) LF4p control, with primary antibody omitted, showing no specific fluorescence. Using Cy3 secondary antibodies, (*E*) shows *lf4* mutant labeled with FLA10p in a punctate pattern and the inset was the *lf4* control with primary antibody omitted, having no specific fluorescence. (*F*) A confluent layer of IMCD cells labeled with α-tubulin primary and showing microtubules throughout the cytoplasm and some discrete points of fluorescence that represent centrioles (black arrowheads). Some images are overexposed to enhance visualization of flagellar staining. All bars are 10 μm.

Scanning Electron Microscopy

The topography of representative *lf4* and wild-type cells (Figure 6, *A*-*C*) appeared similarly oblong. The flagella of *lf4* cells were observed to be grossly longer, as seen in bright-field microscopy. The long flagella were more twisted and folded than wild-type flagella (Figure 6, *B* & *C*). CHO cells showed intact membranes with typical surface

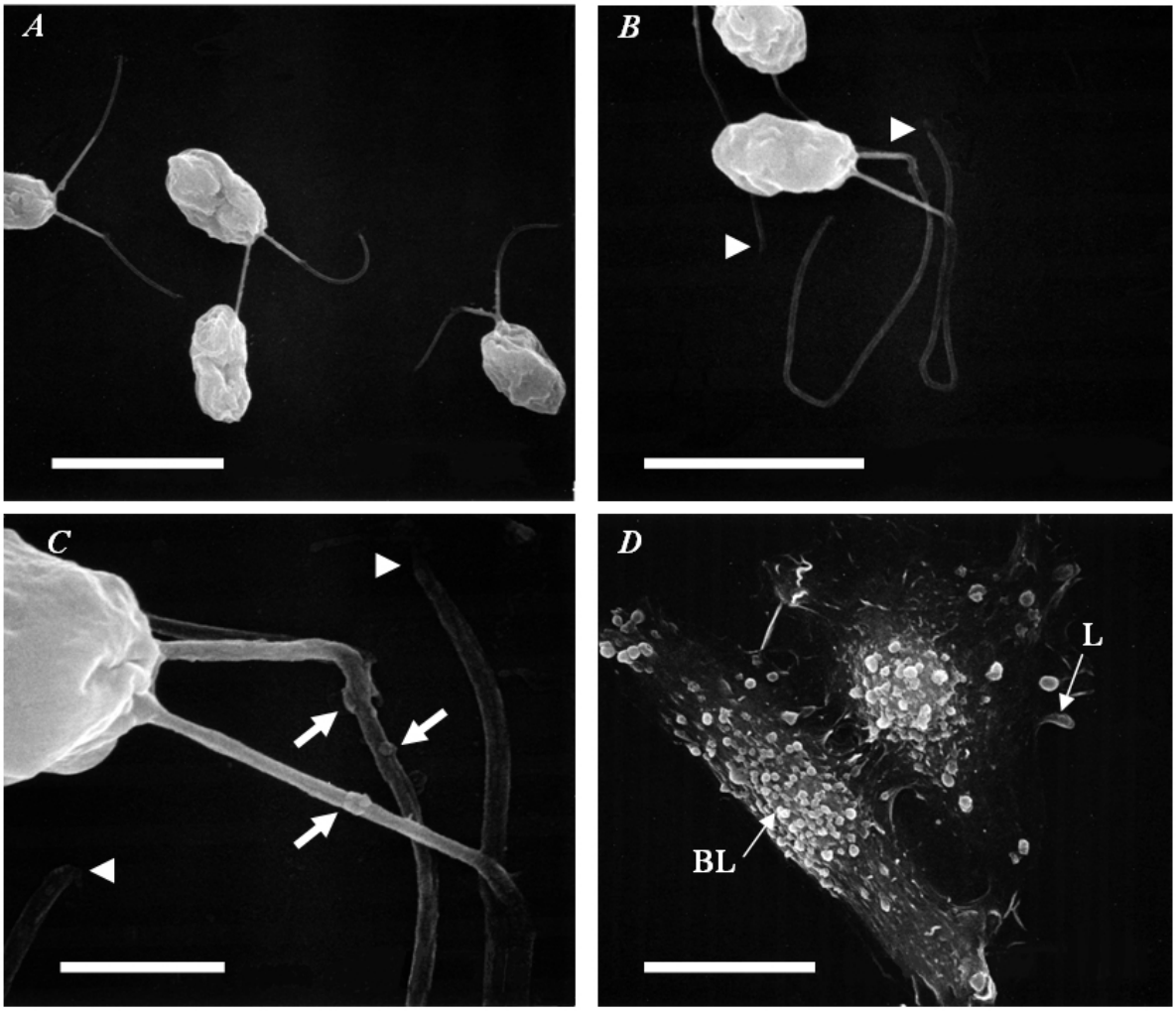

***Figure 6*:** SEM images of *lf4* and wild-type cells. In (*A*), wild-type flagella are approximately the length of a cell body. (*B*) In the *lf4* mutant, the long flagella are apparent and folded back. Note the flagellar tips appear to taper (arrowheads). (*C*) A higher mag of the same *lf4* cell shows some sharply demarcated bulges along the proximal flagellar membrane (thick arrows). (*D*) Two CHO cells show the surface topography features of round, bulbous blebs (BL) and wavy, peripheral lamellipodia (L). Scale bars in (*A*, *B* and *D*) are 10 μm; bar is 2 μm in (*C*).

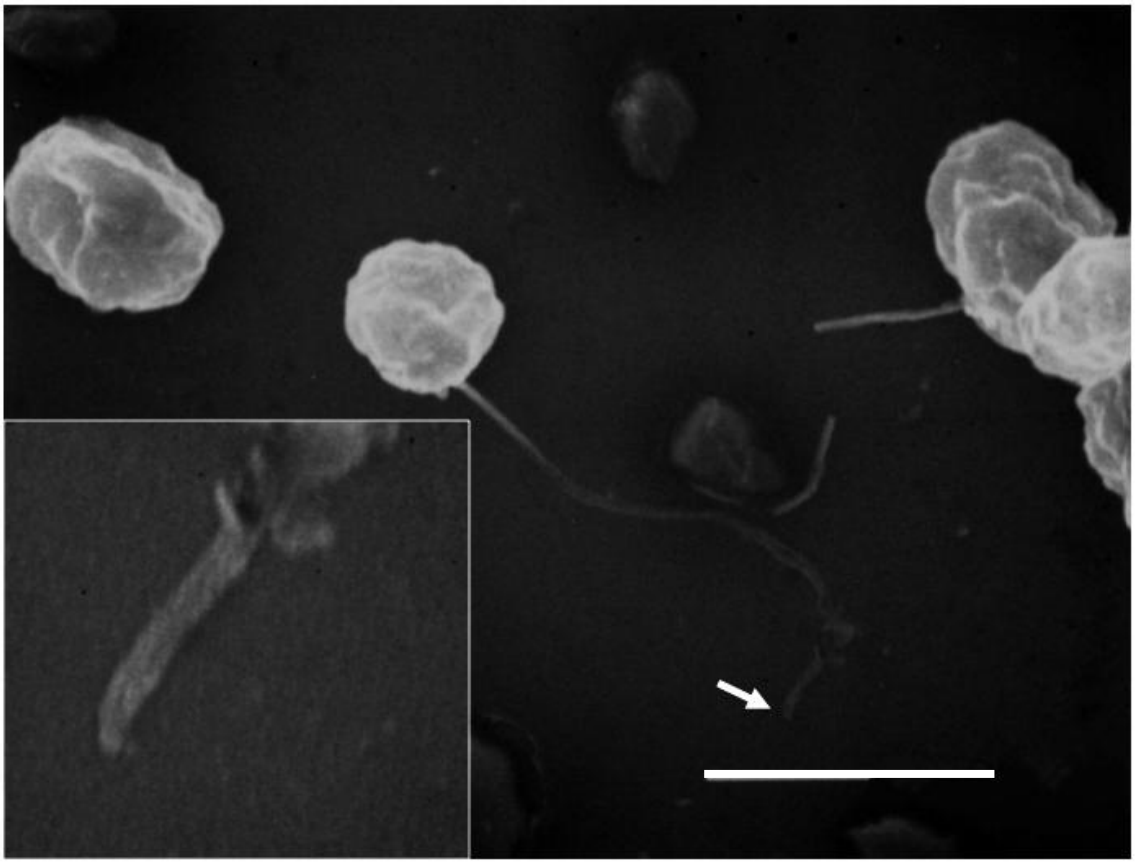

***Figure 7*:** SEM images of *lf4* flagellar tips. The *lf4* flagellar tips (arrow and inset) appear to tapper rather than end in bulbs. Bar is 10 μm.

features (Figure 6, *D*). In contrast to the bulbous ends of flagella with some length control mutants, the tips of *lf4* appeared tapered with no bulbs (Figure 6, *B*-*C*; and Figure 7).

Transmission Electron Microscopy

TEM images demonstrated that *lf4* mutants were similar to wild-type in respect to the cell body structures. The nucleus, nucleolus, chloroplast, ribosomes, mitochondria, and vacuoles appeared undistinguishable from wild-type (Figure 8, *A*-*B*). Both wild-type and *lf4* had centrally located nuclei and chloroplasts that wrapped around in the basolateral and distal ends of the cell body. In the cell apical region, the basal body ultrastructure appeared similar (Figure 8, *C*-*D*). Representative cross-sections and longitudinal profiles of *lf4* flagella demonstrated the 9+2 axoneme ultrastructure with

intact inner and outer dynein arms and radial spokes. The cell membranes enveloping the flagella were intact and IFT particles were seen between the outer-microtubule doublets and the flagellar membranes in both *lf4* and wild-type (Figure 9, *A*-*C*).

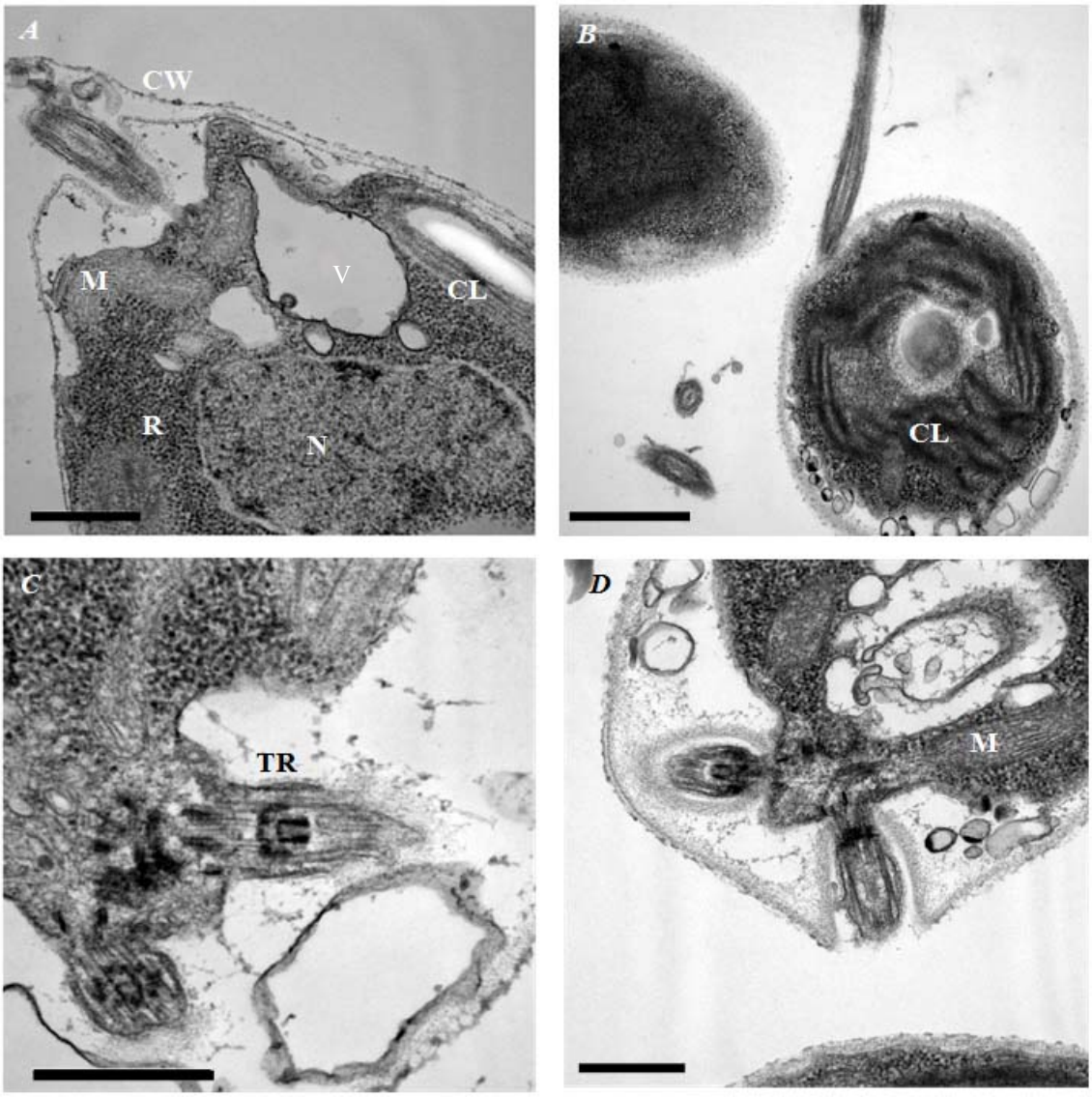

***Figure 8*:** Cell body electron micrographs in *lf4* (*B* and *D*) and wild-type cells (*A* and *C*). In (*A*), a flagellum emerges from the cell wall (CW). Chloroplasts (CL), mitochondria (M), vacuole (V), ribosomes (R), and the nucleus (N) are evident. In (*B*), chloroplasts fill the cell body. The basal body region in (*C*) depicts the transitional region (TR) and in (*D*), the basal body area shows two flagella and some closely related mitochondria. Ribosomes are abundant in the area around the basal bodies as seen in *C* and *D*. Bars are 0.5 µm (*A*), (*C*) and (*D*); and 1 µm in (*B*).

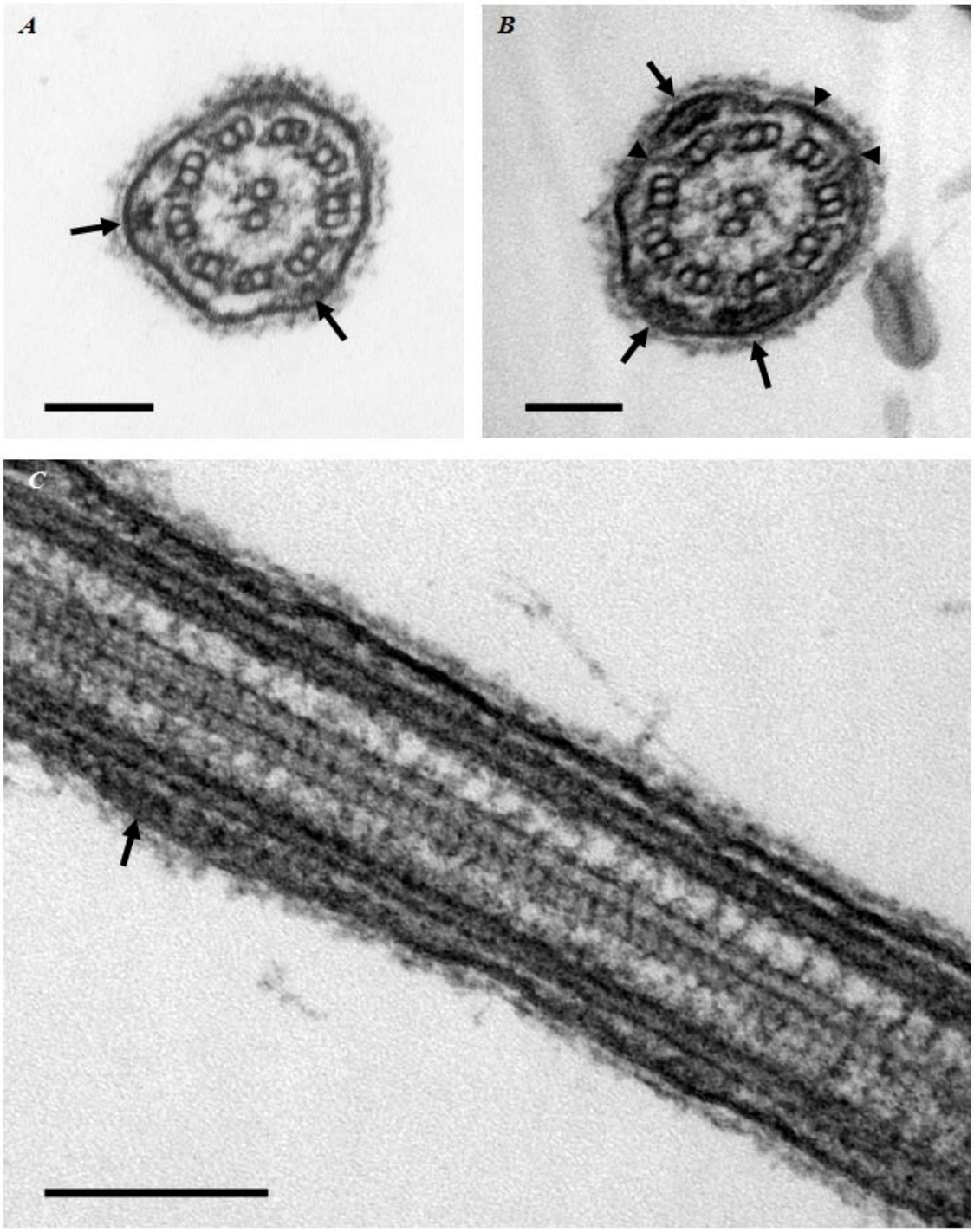

***Figure 9*:** Electron micrographs of flagella found in *lf4* and wild-type cells. The 9+2 microtubule arrangement is apparent in (*A*) wild-type and (*B*) *lf4* cross-sections. IFT particles were seen between the outer-doublet microtubules and the cell membrane with concomitant membrane bulges (arrows). (*B*) An unidentified electron-dense band is seen connecting the *lf4* outer-doublet microtubules to the cell membrane without the membrane bulges (arrowheads). (*C*) A longitudinal view of an *lf4* flagellum with a large IFT raft particle (arrow). Bars are 100 nm (*A*) and (*B*); and (*C*) 200 nm.

The flagellar membrane was always observed as intact over these structures and sometimes appeared to bulge around IFT particles. Interestingly, in one cross-section of the *lf4* axoneme (Figure 9, *B*), an as yet unidentified electron-dense thin band was observed that appeared to connect the outer-doublet microtubules to the cell membrane.

Quantification of IFT Particles

More IFT particles and total flagellar length, area and volume were measured in *lf4* samples (n = 100). However, the same number of IFT particles per total length, area and volume were observed in both wild-type (n = 98) and *lf4*. The mean diameter of flagella appeared relatively equal in both wild-type and *lf4* (Table 3).

	Wild-Type	***lf4***
Total IFT particles	162	234
Total flagellar length (μm)	37.1	52.5
IFTs per length (IFT/μm)	4.4	4.5
Total flagellar area (mm^2)	9.9	14.3
IFTs per area (IFT/mm^2)	16.3	16.3
Total flagellar volume (mm^3)	1737.0	2474.6
IFTs per volume (IFT/mm^3)	.093	.095
Mean diameter of flagella (nm)	240.9 ± 25.9 CI 0.164034	247.9 ± 31.9 CI 0.199749

***Table 3*:** Quantification of IFT particles. Both cross- and longitudinal-sections of wild-type (n = 98) and *lf4* (n = 100) were analyzed for total IFT particles, total length and total diameter. From these measures, IFTs per total area and volume are calculated. Mean flagellar diameter is also reported.

CHAPTER V

DISCUSSION AND CONCLUSION

The purpose of this study was to phenotypically describe the *lf4* mutant of *C. reinhardtii*. *lf4* was morphologically compared to wild-type cells using bright-field, SEM and TEM. IMF was used to localize the FLA10p kinesin-II, which is known to be necessary for assembly and maintenance of flagella (Kozminski et al., 1993). LF4p was also localized. Prior to this study *lf4* cells had not been ultrastructurally characterized.

In culturing of *C. reinhardtii*, wild-type cells were easiest to grow while the *lf4* strains appeared to be more recalcitrant to reaching and maintaining high percentages of swimming cells. Swimming cells typically displayed two flagella, while dividing cells showed lower percentages of activity and no flagella. For example, it was difficult to capture IMF images of *lf4-10*, when only 35% of cultured cells were actively swimming. Nevertheless, all strains of *C. reinhardtii* produced flagella, though not on all cells, that could be found and labeled during microscopic studies.

Why did *lf4* flagella show less of an ability to attain swimming activity? This may be due to several reasons. First the media and cultures were checked for contamination; no signs of bacterial or other contamination were detected in the cultures used in this study. Using a different *C. reinhardtii* mutant, Yang and Yang reported in 2006 that two different *Chlamydomonas* mutants may be highly sensitive to changes in media conditions. Second, the *lf4* strains were mutated cells. This may explain their inability to swim as fast and adept as wild-type, yet this may not satisfactorily explain why the *lf4* cells with long flagella demonstrated low apparent swimming activity. Third, having longer flagella meant that more force was needed to overcome the accumulated

attractions of the glycocalyx to the glass coverslip. So *lf4* would be expected to demonstrate less swimming activity and the minute forces between the glass and glycocalyx may explain the motionless *lf4* flagella. On the other hand, the wild-type strain appeared to have more active cells and generally displayed greater than 50% swimming activity from 24-72 h. Temperature, inoculation concentrations, and light:dark cycles were not altered throughout this study and are not considered to be possible factors influencing *lf4* swimming ability. Additionally, the swimming activity was investigated ad hoc, so it should be noted that *lf4* strains were not always so resistant to start swimming. Temporal or passage factors of maintaining cell strains may also play a role in the swimming percentages. Future research in studying swimming activity using newly acquired strains versus old strains, in a randomized-controlled and blind study may facilitate in answering this question.

Under bright-field microscopy, the wild-type appeared to grossly demonstrate flagella of expected length versus the distinctly longer *lf4* mutant flagella (Asleson and Lefebvre, 1998). Despite lower swimming percentages, the *lf4* cells swam in a characteristic jerky pattern as seen in other *long-flagella* mutants, while the wild-type swimming patterns appeared to be active and without impediment (Asleson and Lefebvre, 1998). The addition of Lugol's iodine stain made flagella more distinct and helped serve as a quick check on approximate length of flagella (Gray, 1954) that helped ensure cultures appeared uniform in length. In conclusion, bright-field microscopy allowed for the gross morphological differences, such as flagellar length and estimated swimming activity, to be catalogued between wild-type and *lf4*.

From the IMF results, the FLA10p kinesin-II showed immunoreactivity in *lf4* along the length of both flagella, in a punctate pattern. Additionally, since FLA10p is known to transport IFT particles in an anterograde fashion, the punctate staining likely represents its presence in these areas for transporting IFT particles. LF4p also was investigated via IMF. This protein was genetically removed to produce the *lf4* mutant. Though captured images contained background staining, this study found LF4p in flagella of wild-type in a punctate pattern and no staining in *lf4* flagella. No staining should occur in the *lf4* because the protein was knocked out, however, some images with extremely high background demonstrated cells with some immunoreactivity. So knowing that if any LF4p signal is observed, then this invalidates a signal seen in wild-type cells. This variation may be due to inadequate washing, though all washing steps consisted of three rounds of 5 min. A likely contributing factor was that the LF4p primary antibody was not diluted in blocking buffer as were all subsequent IMF experiments. The primary antibody itself may have been too concentrated at 1:50 or the secondary antibodies may have been too concentrated. Perhaps all of these possibilities may explain the results observed with LF4p.

Of the secondary antibodies utilized, the Alex Fluor 488-labeled secondary antibody provided the best fluorescence, based on the quality of photographable images. Cy3-labeled secondary antibody yielded good images but with a weaker signal. The Cy3 secondary was received in July 2000 and exceeded the typical shelf-life. However, no major ill effects were observed other than mild attenuation of fluorescence intensity when compared to Alex Fluor 488.

The topographic study of the *lf4* mutant, using SEM, revealed an interesting finding on long flagella. The *lf4* demonstrated long flagella in a folded fashion, but unexpectedly revealed sharply demarcated bulges along the flagella. These bulges could represent IFT and its cargo in the assembly of long flagella. In prior ultrastructural studies using TEM, bulges have been reported at sites of IFT particles, however the images appeared to have smooth demarcations (Cole et al., 1998). I cannot rule out other possibilities that may include artifact, membrane disruption from osmotic effects, or a defective mechanism involved in IFT. These bulges were observed in the proximal region of both wild-type and *lf4* flagella, and if these observations are truly IFT particles, then bulges would likely be observed along the full length. Further research in the assessment of this phenotype in *lf4* mutants may help to identify these structures.

Using SEM images, the *lf4* flagellar tips were noted to differ from other *long-flagellar* mutants, such as *lf2* and *lf3* (Tam et al., 2003; Tam et al. 2007). The tip bulges reported in *lf2* and *lf3* were not observed in *lf4* SEM images, indicating a difference in morphology. The tapering ends of *lf4* flagella indicate the *lf4* mutant assembles or disassembles flagella differently than the *lf2* and *lf3* mutants, in which IFT particles over-accumulate at their bulbous ends, but not apparently so in *lf4* flagella tips. Further SEM characterizations of all four *long-flagellar* mutants would help resolve the differences seen in morphology.

As observed in the cross-sectional and longitudinal electron micrographs, the electron-dense particles are likely IFT particles. These images represent the first ultrastructural analysis of the *lf4* mutant. In comparison to wild-type, the basal bodies and axoneme appeared the same, except for an unidentified thin band connecting the cell

membrane to the outer-doublet microtubules. These bands are still preliminary but appeared at regular intervals surrounding this axoneme. Conversely, these unusual bands were not observed nor have they been reported in wild-type flagella (Harris, 2008b). The bands are as thin as radial spokes, but no spokes have been reported here, nor do spokes originate in this area. Typically, radial spokes originate from the A microtubule and interact with the central pair microtubules. So, these structures may represent an adulteration of the *lf4* axoneme. Other possibilities include artifactual observations or merely the most proximal or distal component of IFT particles. The later seems unlikely, as no similar structure was observed in wild-type axonemes. At this time, more research is needed to determine what these structures may represent.

The significance of morphological assessment of *lf4* flagella was viewed in light of human ciliary disorders. The important connection linking flagella to cilia and the multitude of ciliopathies was reviewed by Pan and Snell (2005). These authors described the role of cilia in sensory perception and how the loss of function leads to disease. Furthermore, they discussed PKD that most commonly strikes in adulthood and is inherited primarily in an autosomal dominant pattern. A less common variant is autosomal recessive and fatal to neonates (Igarashi and Somlo, 2002). The same genes that have been attributed to PKD also are rooted in the genetics encoding primary cilia (Yoder, 2007). Several homologous PKD genes are encoded in *C. reinhardtii* (Pazour, 2008), making it the ideal basic science organism for ciliopathy research.

Chodhari et al. (2004) outlined the pathogenesis of primary ciliary dyskinesia (PCD), another ciliary-related disorder. In PCD, ciliary dysfunction occurs during embryologic development and results in defects in left-right axis patterning (Taulman et

al., 2001), such as formation of dextrocardia, or a right-sided heart. A clinical triad of signs for PCD include: recurrent sinopulmonary disease (such as chronic upper respiratory infections), infertility and the laterality defects such as situs inversus are found in up to 50% of PCD patients (Chodhari et al., 2004). The basic science principles that *C. reinhardtii* offers in researching ciliopathies can facilitate the scientific pursuit of treating PCD, PKD and the other disorders of cilia.

In summary, *Chlamydomonas* represents an ideal organism to investigate IFT, control of flagellar length and the basic science of ciliopathies. Studying *Chlamydomonas* flagella is equivalent to studying cilia and by extension to studying primary cilia. This study observed that the *lf4* flagella were grossly longer than wild-type and demonstrated low percentages of swimming cells. FLA10p was labeled and localized to the flagella of wild-type and *lf4* in a punctate pattern. The observation that the flagella of *lf4* are tapered at their tips is in contrast to previous studies of *lf2* and *lf3* that form bulges at the tips of their flagella. The ultrastructure of *lf4* revealed IFT particles and the presence of an unidentified structure between the outer-doublet microtubules and the cell membrane. The number of IFT particles per total length was the same in wild-type and *lf4* suggesting they operate independently and confirms my hypothesis. Localization with immunogold electron microscopy is the logical next step in furthering this phenotypic study of IFT transport and FLA10p in the *lf4* mutant of *C. reinhardtii*.

References

Alberts, B., A. Johnson, J. Lewis, M. Raff, K. Roberts, and P. Walter. 2008. The Cytoskeleton. *In* Molecular Biology of the Cell. B. Alberts, editor. Garland Science, Oxford, UK. 1031-1035.

Asleson, C.M., and P.A. Lefebvre. 1998. Genetic Analysis of Flagellar Length Control in *Chlamydomonas reinhardtii*: A New *Long-Flagella* Locus and Extragenic Suppressor Mutations. *Genetics.* 148:693-702.

Berman, S.A., N.F. Wilson, N.A. Haas, and P.A. Lefebvre. 2003. A Novel MAP Kinase Regulates Flagellar Length in *Chlamaydomonas*. *Curr Biol.* 13:1145-1149.

Caprette, D.R. 1996. Fixing *Chlamydomonas* to observe and preserve flagella. *online*: http://www.ruf.rice.edu/~bioslabs/studies/invertebrates/chlamfix.html. Updated in 2006 and accessed April 1, 2009:1-3.

Carson, F.L., J.H. Martin, and J.A. Lynn. 1973. Formalin Fixation for Electron Microscopy: A Re-evaluation. *Am J Clin Pathol.* 59:365-373.

Chodhari, R., H. Mitchinson, and M. Meeks. 2004. Cilia, primary ciliary dyskinesia and molecular genetics. *Paediatr Respir Rev.* 5:69-76.

Cole, D.G. 1999. Kinesin-II, the heteromeric kinesin. *Cell Mol Life Sci.* 56:217-226.

Cole, D.G., D.R. Diener, A.L. Himelblau, P.L. Beech, J.C. Fuster, and J.L. Rosenbaum. 1998. *Chlamydomonas* Kinesin-II-dependent Intraflagellar Transport (IFT): IFT Particles Contain Proteins Required for Ciliary Assembly in *Caenorhabditis elegans* Sensory Neurons. *JCB.* 141:993-1008.

Dentler, W.L. and C. Adams. 1992. Flagellar Microtubule Dynamics in *Chlamydomonas*: Cytochalasin D Induces Periods of Microtubule Shortening and Elongation; and cochicine induces disassembly of the distal, but not proximal, half of the flagellum. *JCB*. 117:1289-1298.

Domozych, D.S. 1999. Disruption of the Golgi apparatus and secretory mechanism in the desmid, *Closterium acerosum*, by brefeldin A. *J Exp Biol.* 50:1323-1330.

Geimer, S., and M. Melkonian. 2004. The ultrastructure of the *Chlamydomonas reinhardtii* basal apparatus: identification of an early marker of radial asymmetry inherent in the basal body. *J. Cell Sci.* 117:2663-2674.

Gorman, D.S., and R.P. Levine. 1965. Cytochrome F and Plastocyanin: Their Sequence in the Photosynthetic Electron Transport Chain of *Chlamydomonas reinhardtii*. *Proc Natl Acad Sci USA.* 54:1665-1669.

Gray, P. 1954. The Microtomist's Formulary and Guide. R E Krieger Pub Co, Huntington, NY. 680 pp.

Harlow, E., and D. Lane. 1988. Antibodies: A Laboratory Manual. Cold Spring Harbor Laboratory Press, Woodbury, NY. 726 pp.

Harris, E.H. 2008a. The Genus *Chlamydomonas*. *In* The *Chlamydomonas* Sourcebook, Volume 1. E.H. Harris, editor. Elsevier/Academic Press, Burlington, MA. 1-24.

Harris, E.H. 2008b. Motility and Behavior. *In* The *Chlamydomonas* Sourcebook, Volume 1. E.H. Harris, editor. Elsevier/Academic Press, Burlington, MA. 89-117.

Hayflick, L. 1961. The Establishment of a Line (WISH) of Human Amnion Cells in Continuous Cultivation. *Exp Cell Res.* 23:14-20.

Huang, B., D.M. Watterson, V.D. Lee, and M.J. Schibler. 1988. Purification and Characterization of a Basal Body-associated Ca^{2+}-binding Protein. *JCB.* 107:121-131.

Igarashi, P., and S. Somlo. 2002. Genetics and Pathogenesis of Polycystic Kidney Disease. *J Am Soc Nephrol.* 13:2384-2394.

Kierszenbaum, A.L. 2007. Epithelium. *In* Histology and Cell Biology. A.L. Kierszenbaum, editor. Elsevier/Mosby, New York, NY.

Kozminski, K.G., K.A. Johnson, P. Forscher, and J.L. Rosenbaum. 1993. A motility in the eukaryotic flagellum unrelated to flagellar beating. *Proc Natl Acad Sci USA.* 90:5519-5523.

Lefebvre, P.A. 2008. Flagellar Length Control. In The *Chlamydomonas* Sourcebook Volume 3. G.B. Witman and E.H. Harris, editors. Elsevier/Academic Press, Burlington, MA. 115-129.

Malone, A.M., C.T. Anderson, P. Tummala, R.Y. Kwon, T.R. Johnston, T. Stearns, C.R. Jacobs. 2007. Primary cilia mediate mechanosensing in bone cells by a calcium-independent mechanism. *Proc Natl Acad Sci USA.*104:13325-13330.

Marshall, W.F., H. Qin, M.R. Brenni, and J.L. Rosenbaum. 2005. Flagellar Length Control System: Testing a Simple Model Based on Intraflagellar Transport and Turnover. *Mol Biol Cell.* 16:270-278.

Marshall, W.F., and J.L. Rosenbaum. 2001. Intraflagellar transport balances continuous turnover of outer doublet microtubules: implications for flagellar length control. *JCB.* 155:405-414.

Meek, W.D., and W.L. Davis. 1986. Fine structure and immunofluorescenct studies of the WISH cell line. *In Vitro Cell Dev Biol.* 22:716-724.

Michaud, E.J. and B.K. Yoder. 2006. The Primary Cilium in Cell Signaling and Cancer. *Cancer Res*. 66:6463-6467.

Miller, K.E., B.A. Richards and R.M. Kreibal. 2002. Glutamine-, glutamine synthetase-, glutamine dehydrogenase- and pyruvate carboxylase-immunoreativities in the rat dorsal root ganglion and peripheral nerve. *Brain Res*. 945:202-211.

Mueller, J., C.A. Perrone, R. Bower, D.G. Cole, and M.E. Porter. 2005. The *FLA3* KAP Subunit Is Required for Localization of the Kinesin-2 to the Site of Flagellar Assembly and Processive Anterograde Intraflagellar Transport. *Mol Biol Cell.* 16:1341-1354.

Nguyen, R.L., L.W. Tam, and P.A. Lefebvre. 2004. The *LF1* Gene of *Chlamydomonas reinhardtii* Encodes a Novel Protein Required for Flagellar Length Control. *Genetics.* 169:1415-1424.

Pan, J., and W.J. Snell. 2005. *Chlamydomonas* Shortens Its Flagella by Activating Axonemal Disassembly, Stimulating IFT Particle Trafficking, and Blocking Anterograde Cargo Loading. *Dev Cell.* 9:431-438.

Pan, J., and W.J. Snell. 2002. Kinesin-II Is Required for Flagellar Sensory Transduction during Fertilization in *Chlamydomonas*. *Mol. Biol. Cell.* 13:1417-1426.

Pazour, G.J. 2004. Intraflagellar Transport and Cilia-Dependent Renal Disease: The Ciliary Hypothesis of Polycystic Kidney Disease. *J Am Soc Nephrol.* 15:2528-2536.

Pazour, G.J., and G.B. Witman. 2008. The *Chlamydomonas* Flagellum as a Model for Human Ciliary Disease. *In* The *Chlamydomonas* Sourcebook, Volume 3. G.B. Witman and E.H. Harris, editors. Elsevier/Academic Press, Burlington, MA. 445-468.

Pederson, L.B. and J.L. Rosenbaum. 2008. Intraflagellar Transport (IFT): Role in Ciliary Assembly, Resorption and Signaling. *Curr Top Dev Biol.* 85:23-61.

Puck, T.T., S.J. Cieciura, and A. Robinson. 1958. Genetics of Somatic Mammalian Cells, III. Long-Term Cultivation of Euploid Cells from Human and Animal Subjects. *J Exp Med.* 108:945-956.

Qin, H., D.R. Diener, S. Geimer, D.G. Cole and J.L. Rosenbaum. 2004. Intraflagellar transport (IFT) cargo: IFT transports flagellar precursors to the tip and turnover products to the cell body. *JCB* 164:255-266.

Rauchman, M.I., S.K. Nigam, E. Delpire, and S.R. Gullan. 1993. An osmotically tolerant inner medullary collecting duct cell line from an SV40 transgenic mouse. *Am J Physiol.* 265:F416-F424.

Sager, R., and S. Granick. 1954. Nutritional control of sexuality in *Chlamydomonas reinhardi*. *J Gen Physiol.* 37:729-742.

Tam, L.W., W.L. Dentler, and P.A. Lefebvre. 2003. Defective flagellar assembly and length regulation in *LF3* null mutants in *Chlamydomonas*. *JCB*. 163:597-607.

Tam, L.W., N.F. Wilson, and P.A. Lefebvre. 2007. A CDK-related kinase regulates the length and assembly of flagella in *Chlamydomonas*. *JCB.* 176:819-829.

Taulman, P.D., C.J. Haycraft, D.F. Balkovetz, and B.K. Yoder. 2001. Polaris, a Protein Involved in Left-Right Axis Patterning, Localized to Basal Bodies and Cilia. *Mol Biol Cell.* 12:589-599.

Wilson, N.F., J.K. Iyer, J.A. Buchheim, and W.D. Meek. 2008. Regulation of flagellar length in *Chlamydomonas*. *Semin Cell Dev Biol.* 19:494-501.

Yang, C., and P. Yang. 2006. The flagellar motility of *Chlamydomonas* pf25 mutant lacking an AKAP-binding protein is overtly sensitive to medium conditions. *Mol Biol Cell.* 17:227-238.

Yoder, B.K. 2007. Role of Primary Cilia in the Pathogenesis of Polycystic Kidney Disease. *J Am Soc Nephrol.* 18:1381-1388.

Zimmerman, K.W. 1898. Contributing to the knowledge of glands and epithelium. *Arch Mikr Entwicklungsmech*. 52:552-706.

APPENDIX

A. Growth Experiment Video: *C. reinhardtii* wild-type and several *lf4* strains were analyzed for percent of cells swimming per time in March 2009.

B. A Video on 'How to Operate the OSU-CHS Zeiss T109 Electron Microscope' by Kevin Pargeter

VITA

Kevin Matthew Pargeter

Candidate for the Degree of Master of Science

Thesis: A PHENOTYPIC STUDY OF INTRAFLAGELLAR TRANSPORT AND FLA10 IN THE *lf4* MUTANT OF *CHLAMYDOMONAS REINHARDTII*

Major Field: Biomedical Science

Biographical:

Born in 1979 to Terry and Carolyn Pargeter, I was the fourth of six children to be raised in Oklahoma City, OK. Professionally my interests lie within the field of Internal Medicine and the basic science of ciliary disorders, called ciliopathies. Specifically, using the green alga *Chlamydomonas reinhardtii*, which has been established as the model organism for ciliopathies (Pazour 2004), I have gained a fruitful series of academic experiences in biomedical research. From the result of pursing a Master of Science concurrent with the third and fourth years of medical school, this education has greatly enriched my life and sharpened my academic goals. Ultimately, experimental and clinical techniques in transmission, scanning and immunofluorescent microscopy have become tools of my research efforts. With a D.O./M.S. education, I will pursue an internal medicine academic position at a medical center that involves responsibilities in teaching, research and patient care.

Education:

1. Expecting Doctor of Medicine at Oklahoma State University College of Osteopathic Medicine, Tulsa, OK, on May 15, 2009.
2. Expecting Master of Science at Oklahoma State University Center for Health Sciences, Tulsa, OK, on May 15, 2009.
3. Bachelor of Science in Biology at the University of Central Oklahoma, Edmond, OK, on May 2004, *Cum laude*.

Experience:

1. Teacher Asst, Histology Tutor & Researcher. OSU-CHS, Tulsa, May-Dec 2006.
2. U.S. Senate Intern for Senator Jim Inhofe, Washington, D.C., May-June 2004.
3. Undergrad Research Asst, UCO, Edmond, OK, Aug 2004-May 2005.

Professional Memberships: AMA, ACP, AOA, Sigma Xi, Oklahoma Microscopy Society and Oklahoma Academy of Science.

Name: Kevin Matthew Pargeter **Date of Degree:** May 2009

Institution: Oklahoma State University Center for Health Sciences, Tulsa, Oklahoma

Title of Study: A PHENOTYPIC STUDY OF INTRAFLAGELLAR TRANSPORT AND FLA10 IN THE *lf4* MUTANT OF *CHLAMYDOMONAS REINHARDTII*

Pages in Study: 35 Candidate for the Degree of Master of Science

Major Field: Biomedical Science

Scope and Method of Study:

Chlamydomonas reinhardtii is a biflagellate, unicellular green alga that serves as an ideal basic science organism (Harris, 2008a). Compared to eukaryotic primary cilia, it shares many homologous flagellar genes with humans, of which several ciliary disorders, or ciliopathies, are known to occur (Pazour, 2008). Almost all vertebrate cells possess primary cilia, but this organelle had long been thought to have no function (Pan et al., 2005). With the discovery of intraflagellar transport (IFT), the mechanism for flagellar assembly, by Kozminski and coworkers (1993), new approaches to study ciliopathies were established. To investigate how flagellar length was controlled, *long-flagellar* mutants *lf1*, *lf2*, *lf3* and *lf4* were created. Yet little phenotypically was known about *lf4*. To characterize the morphology of and localize IFT proteins (FLA10p and LF4p) in the *lf4* mutant, this work used bright-field microscopy, immunofluorescence microscopy (IMF), scanning electron microscopy (SEM) and transmission electron microscopy (TEM).

Findings and Conclusions:

The *lf4* flagella were grossly longer than wild-type cells, which were observed to be most active at 36 h. The *lf4* cells were most active between 24-36 h likely indicating the best time to harvest for experimentation. Using IMF, the FLA10p and LF4p localized to flagella in a punctate pattern, likely indicating IFT particles. No bulbous tips were observed in *lf4*, unlike the *lf2* and *lf3* mutants as reported by Tam and coworkers (2003; 2007). Multiple IFT particles were observed in cross-sectional and longitudinal flagellar ultrastructure of *lf4* using TEM. Plus, an as yet unidentified electron-dense structure in an *lf4* cross-section was observed to connect the outer doublet microtubules to the cell membrane. Quantification of IFT particles per length, area and volume of flagella were the same in wild-type and *lf4*, suggesting that IFT particle quantity is independent of length. Immunogold electron localization is the logical next step to further the phenotypic characterization of the *lf4* mutant.

ADVISER'S APPROVAL: _____

William D. Meek, Ph.D.